An algorithm for the kinetics of tire pyrolysis under different heating rates

Augustine Quek, Rajashekhar Balasubramanian*

Division of Environmental Science & Engineering, Faculty of Engineering, National University of Singapore, Block EA #03-12, 9 Engineering Drive 1, Singapore 117576, Singapore

A B S T R A C T

Tires exhibit different kinetic behaviors when pyrolyzed under different heating rates. A new algorithm has been developed to investigate pyrolysis behavior of scrap tires. The algorithm includes heat and mass transfer equations to account for the different extents of thermal lag as the tire is heated at different heating rates. The algorithm uses an iterative approach to fit model equations to experimental data to obtain quantitative values of kinetic parameters. These parameters describe the pyrolysis process well, with good agreement ($r^2 > 0.96$) between the model and experimental data when the model is applied to three different brands of automobile tires heated under five different heating rates in a pure nitrogen atmosphere. The model agrees with other researchers' results that frequencies factors increased and time constants decreased with increasing heating rates. The model also shows the change in the behavior of individual tire components when the heating rates are increased above $30\,\mathrm{K\,min^{-1}}$. This result indicates that heating rates, rather than temperature, can significantly affect pyrolysis reactions. This algorithm is simple in structure and yet accurate in describing tire pyrolysis under a wide range of heating rates (10–$50\,\mathrm{K\,min^{-1}}$). It improves our understanding of the tire pyrolysis process by showing the relationship between the heating rate and the many components in a tire that depolymerize as parallel reactions.

© 2008 Elsevier B.V. All rights reserved.

1. Introduction

It is estimated that worldwide, over one billion waste tires are generated annually [1]. Tires do not break down easily in the natural environment. The vulcanized rubber consists of long chain polymers (isoprene, butadiene, and styrene-butadiene) that are cross-linked with sulfur bonds and are further protected by antioxidants and antiozonants that resist degradation. In landfills, rubber tires tend to float to the top due to trapped gases, thus breaking landfill covers. Combustion of tires produces pollutants harmful to human health including polycyclic aromatic hydrocarbons (PAHs), benzene, styrene, phenols, and butadiene [2]. This has put undue demands on conventional disposal options of scrap tires such as landfills and incineration.

Consequently, there is an urgent need for the recycling of scrap tires, especially recovery of valuable resources from this carbonaceous material. Pyrolysis is a feasible method for recovering valuable products such as char, activated carbon, oil and gas from scrap tires [3]. Pyrolysis can be thought of as the thermal breakdown of organic polymers into simpler molecules in the absence of air. Various processes are thought to occur that occur simultaneously such as thermal depolymerization, decomposition, and gasification ([3], and references therein). However, although several fundamental studies on pyrolysis of scrap tires have been carried out over the years ([3], and references therein), the mechanisms involved in the pyrolysis process are not completely understood yet.

Modeling the kinetics of the tire thermal degradation process can provide insights into the mechanisms responsible for tire pyrolysis and predict potential difficulties in a pyrolysis reactor. Earlier studies have built pyrolysis models based on data obtained from thermogravimetry techniques [3], which measures the sample mass loss with time and temperature. One method is to assume a single peak and apply only one set of kinetic parameters [4–8]. For example, Koreňovaï et al. modeled the overall pyrolysis of scrap tires as a single reaction proceeding in two stages [8] using the Arrhenius equation. However, their thermogravimetric (TG) data, showed two maxima in the rate of mass loss for tire pyrolysis. They attributed these two points to lower molecular mass compounds release in the first stage and aromatic and heavier hydrocarbons in the second [8].

The fact that tire pyrolysis is a multi-stage, multi-component phenomenon is widely accepted [9–17]. The first stage of the pyrolysis is attributed to extender oils and softeners, the second stage to isoprene rubber or natural rubber (NR), butadiene (BR) and styrene-butadiene rubbers (SBR) [3,8,10,12,15–18]. Thus, a more realistic and popular approach is to model each major component of the tire separately [9–15]. Each component is represented by a peak in the TG curve, to which the Arrhenius type equation can be fitted. This produces one set of kinetic parameters for each component of the tire being pyrolyzed. The different sets of parameters thus give specific

* Corresponding author. Tel.: +65 6516 5135; fax: +65 6516 5266.
  E-mail address: eserbala@nus.edu.sg (R. Balasubramanian).

Nomenclature

A	preexponential factor ($1\,s^{-1}$)
A_i	preexponential factor for component i ($1\,s^{-1}$)
$E_{a,i}$	activation energy for reaction of component I ($J\,mol^{-1}$)
m_i	mass of component i of the tire (mg)
$m_{i,o}$	initial mass of component i (mg)
m_i^n	mass of component i of the tire (mg) with nth order reaction rate.
M	total mass of tire sample (mg)
N	total number of components evolving independently
r	time constant ($1\,s^{-1}$)
R	molar gas constant ($8.314\,J\,mol^{-1}\,K^{-1}$)
T	global temperature (K)
$T(t)$	temperature of component at time t (K)
$T(0)$	initial temperature (K)
T_f	furnace temperature (K)
t	time of reaction (s)
$x_{i,t}$	mass fraction of a component i at time t

information on the kinetic behavior of the different compounds during the pyrolysis process. This "multi-component" approach to simulate the TG curve is also able to rapidly identify and quantify the rubbers in a material mixture for tire, as this study will show.

However, the extent of tire devolatilzation depends not only on temperature but also on heat transfer by conduction, as shown most recently by Chinyama and Lockwood [19]. A limitation in the pyrolysis modeling efforts conducted so far is the lack of consideration for heat and mass transfer in a kinetics model. One notable exception is a transient 'bubble' model of a single tire particle developed by Yang et al. [20]. The model attempts to predict the temperature gradient through the particle and the subsequent volatile loss, but is not easily scalable to large masses of particles. A full consideration of heat and mass transfer processes is important because tire decomposition during pyrolysis is initially rate-controlled due to predominance of surface reactions, but becomes more diffusion controlled in the final stages [7].

To describe tire pyrolysis more accurately, the algorithm proposed in this work which includes two equations, one to account for heat conduction from the exterior to the interior of the tire particle, and the other for mass transfer from within the tire particle to the surface. By accounting for both reaction rates and heat transfer limitations, the multi-component model is able to decouple each decomposing fraction as an independent parallel reaction from other fractions [15], for both low and high heating rates. Although the model is kept simple for quick simulation to obtain results, it is based only on TG data, for three brands of tires and on heating rates within the range of 10–50 K min^{-1}.

In this paper, kinetic parameters are obtained for tire pyrolysis with the model developed in this study. The corresponding activation energies, preexponential factors, and characteristic parameters were determined for the range of experimental conditions to prove the flexibility of the model. The implications of these results are also discussed.

2. Experimental

2.1. Material

Raw scrap tire samples were obtained from a commercial recycler. The tire samples were cut to small cubes (∼1 mm) and weighed (5–10 mg) prior to each run. The tire cubes were further heated at approximately 104 °C for a few minutes to remove moisture content before starting each run. Three different brands of automobile tires were used in this study (labeled brand 1, 2 and 3). Several runs were done for each tire, with all samples taken from the tire tread. For the tires used the proximate content is: 1–1.2% water, 62–67% volatile carbon, 30–35% fixed carbon, and 2.5–3% ash. Although these values are close to the findings of previous researchers [4,5,7,10,11,18,19], the range of values obtained showed that different tire samples have slightly different compositions and masses. Hence the model should be run for each sample separately, but these differences are expected to be small, as will be shown in the following sections.

2.2. Thermogravimetric analyzer (TGA) measurements

A Shimadzu DTG-60 thermogravimetric analyzer was used to simultaneously measure the temperature and weight of the sample as it was heated up under the N$_2$ atmosphere. The nitrogen gas flow rate was set at 150 ml min^{-1} and the maximum temperature was 800 °C. TGA data were captured every second on the accompanying software. These data were used as input data for the pyrolysis model.

2.3. Kinetic model

Current modeling efforts have focused only on the chemical reactions rates [2,5,6], which implicitly assume a reaction rate limiting mechanism in the pyrolysis of tires. The model used in this study assumes that the tires used composed of only extender oil, natural rubber (NR) and manufactured rubbers (SBR, BR), and each of these components follows the basic Arrhenius-type rate equation with the first order reaction in the pyrolysis process. The activation energies are fixed and unique to each component, using the values obtained by Yang et al. [21] and reproduced in Table 1.

The overall equation is:

$$\frac{dM}{dT} = \sum_{i=1}^{N} m_i k_i \tag{1}$$

where dM/dT is the rate of change of the total mass of the tire sample with change in temperature, N is the total number of components evolving independently, $m_i^n k_i$ is reaction rate of the ith component, with k_i being Arrhenius-type kinetic reaction coefficient of component i expressed as follows:

$$k_i = \frac{dt}{dT} A_i e^{-E_{a,i}/RT} \tag{2}$$

Here dt/dT is the inverse of the heating rate, set at the beginning of each run, and A is the preexponential factor, also known as the frequency factor, $E_{a,i}$ is the activation energy of the particular reaction, R is the molar gas constant ($8.314\,J\,mol^{-1}\,K^{-1}$) and T the temperature of the particular data point. The Arrhenius equation ($A_i e^{-E_{a,i}/RT}$) is multiplied by the inverse of the heating rate (dt/dT) because the rate of mass change with respect to temperature is used (dt/dT).

Table 1
Activation Energies of major tire components [21].

Component	E_a ($kJ\,mol^{-1}$)
Extender oil	43.3/48
NR	207
SBR	152
BR	215

For higher heating rates, thermal lag is modeled by adding the following two equations:

$$T(t) = T_f + (T(0) - T_f)e^{-rt} \tag{3}$$

$$m_i = m_{i,o} 4(x_i)[-\ln(x_i)]^{3/4} \tag{4}$$

Eq. (3) is simplified form of Newton's heat transfer equation [22], where $T(t)$ is the temperature at time t for each data point, T_f is the furnace temperature, external to the rubber sample, and r is the time constant characteristic of the system. Eq. (4) is the third Order Avrami-Erofe'ev equation for bubble growth. $x_{i,t}$ is the mass fraction of a component i at temperature T.

Mass balance was done using

$$m_i = m_{i,o} + \frac{dm_i}{dT}\Delta T \tag{5}$$

where ΔT is the difference in the temperatures between the two data points.

This requires that the initial and final masses be known in order for various m_i to be substituted to start the modeling process. Thus, the thermal rate of mass change with temperature is plotted (dt/dT vs T) where the area under the curve would give an initial estimate of the corresponding component. This is not a common practice. Instead, temporal mass variation (dM/dT) is often plotted against temperature, and an integral function is used to approximate the integral rate equation $\left(\int Ae^{-Ea/RT}dT\right)$ [4–6,10,12,13,17,21,23].

There are several assumptions made in the development and application of this model:

(i) The reaction rate function, representing the rate of reactant mass loss, follows an order of reaction, i.e. $r = km^n$
(ii) The order of reaction n is assumed to be 1.
(iii) The activation energies (E_a) of the main components are fixed for each compound, as given in Table 1.
(iv) When high heating rates are used (30 °C min^{-1} or more), the additional peaks other than the two main peaks are due to high thermal lag, and modeled with the addition of Eqs. (4) and (5).

Non-linear regression was used to obtain the kinetic constants for all cases. The correlation coefficient was calculated using the relation

$$\text{correl} =$$
$$\frac{\sum (dM/dT_{exp\ t} - \overline{dM}/dT_{expt})(dM/dT_{model} - \overline{dM}/dT_{model})}{\sqrt{\sum (dM/dT_{exp\ t} - \overline{dM}/dT_{expt})^2 \sum (dM/dT_{model} - \overline{dM}/dT_{model})^2}} \tag{6}$$

The correlation was done for both the rate of mass loss (dM/dT) data with the model above, and the total mass fraction evolved (fractional conversion) with time. The latter was done by total-
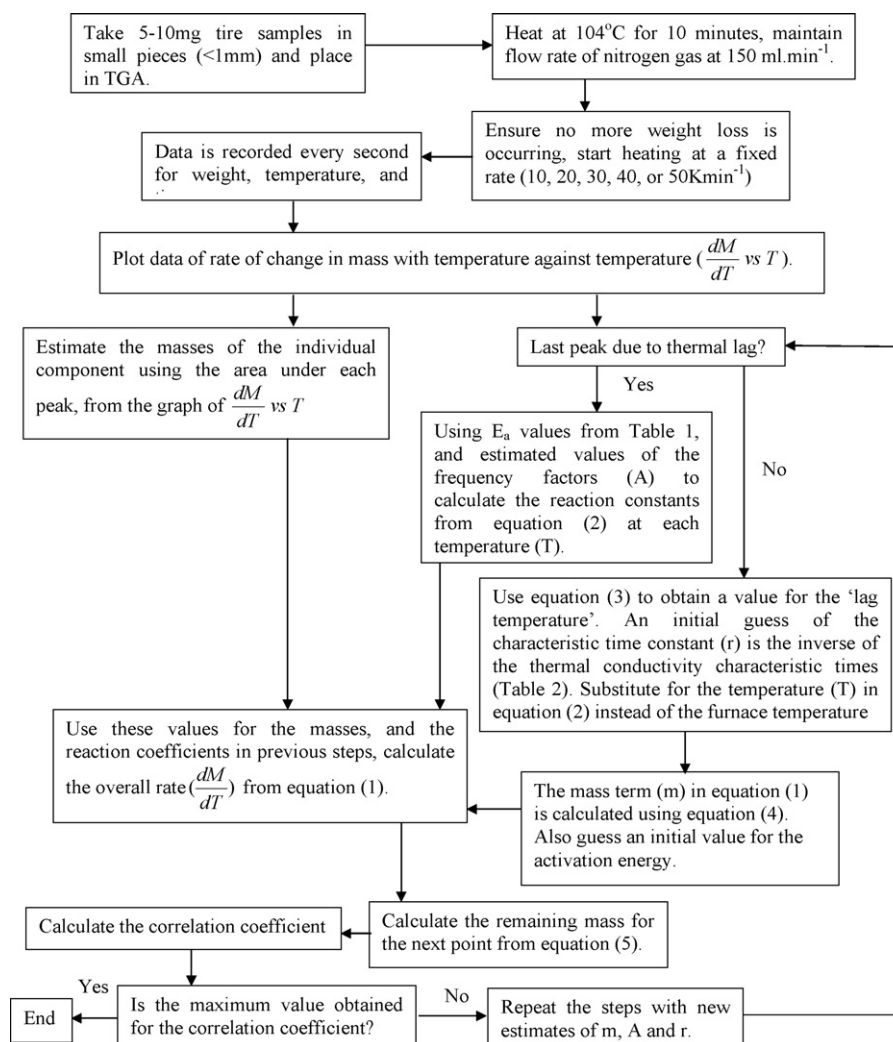

Fig. 1. Flowchart for the entire experimental and modeling procedure in this study.

Table 2
Characteristic times for various heat transfer processes.

Process	Characteristic times (s)	Reference	r (s^{-1})
Tar transport	10^5	[24]	10^{-5}
Conductive heat transfer	10^4	[25]	10^{-4}
Tire pyrolysis ($1/k$)	10^2	[25]	10^{-2}
Viscous flow	10	[26]	10^{-1}

ing all the mass at any time ($\sum_i^N m_i$) and dividing by the initial mass (M), and correlating with the mass fraction calculated from experimental data.

The following steps can be used,

1. Using E_a values from Table 1, and estimated values of the frequency factors to calculate the reaction constants from Eq. (2) for each temperature (T).
2. Estimate the masses of the individual component from the graph of dM/dT vs T.
3. Use these values for the masses, and the reaction coefficients in step 1, calculate the overall rate (dM/dT) from Eq. (1).
4. Calculate the remaining mass for the next point from Eq. (5).
5. Check the correlation coefficient and repeat the steps until the maximum value is obtained for it.
6. For peaks arising due to thermal lag, Eq. (3) is necessary to obtain a value for the 'lag temperature', or the temperature within the tire due to insufficient time for heat transfer. An initial guess of the characteristic time constant (r) in the range of 10^{-2} to 10^{-4} s^{-1} can be used, as the inverse of the thermal conductivity characteristic times (Table 2).
7. This is then substituted for the temperature (T) in Eq. (2) instead of the furnace temperature. The mass term (m) in Eq. (1) is then calculated using Eq. (4) instead. An initial guess for the activation energy would also be required in this case.
8. The whole procedure can be iterated quickly using any mathematical computer software, and initial estimates can even be automatically adjusted in applying the software to do non-linear regression.

A flowchart of the entire procedure, experimental and modeling, is given in Fig. 1.

3. Results and discussion

3.1. TGA modeling and results

Figs. 2 and 3 show the thermal degradation of a tire sample at a heating rate (dT/dt) of 10 K min^{-1} and 20 K min^{-1}, respectively. The degradation rates of the various components, and the net effect, as computed from the model, are shown in these figures. The kinetic constants are presented in Table 3 and the corresponding weight fractions shown in Table 4. Although the experimental data show a fair amount of scatter, a high degree of fit was found (>0.96) for the model to the data (Table 5).

At these heating rates, the degradation of the tire was not inhibited by mass transfer, as seen in the curves. One consequence of this model is that under this condition, the mass fractions from the same brand of tire should be similar (Table 4). There should also be an increase in the frequency factors of each component as heating rates increase. Only at higher heating rates can the reactions curve for mass transfer be seen (Figs. 4–8), which can be modeled as a separate, parallel reaction from the other components.

Tables 3–5 also give the various values of kinetic parameters, tire component mass fractions, and goodness of fits, obtained from the model for higher heating rates of three different brands of tires. The
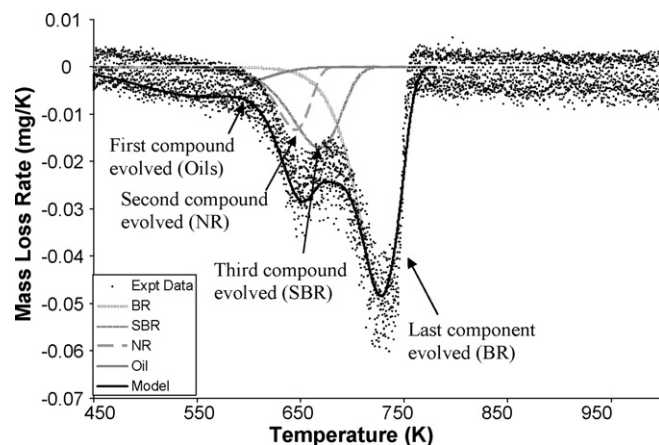

Fig. 2. Deconvolution of different components of the tire brand 1 at dT/dt = 10 K min^{-1}.
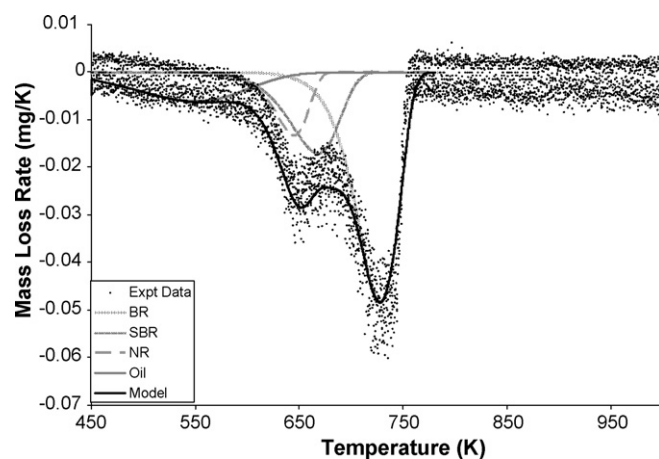

Fig. 3. Deconvolution of different components of the tire brand 1 at dT/dt = 20 K min^{-1}.

graphical results for one brand of tire at three different high heating rate s are shown in Figs. 4–6.

Thermal lag in pyrolysis can be seen in these derivative thermogravimetry (DTG) curves as a small peak towards the end of the pyrolysis process. Reactions of compounds that could not keep up with the thermal ramp rate would show up as a much smaller peak on the DTG curve. This may be attributed to the evolu-
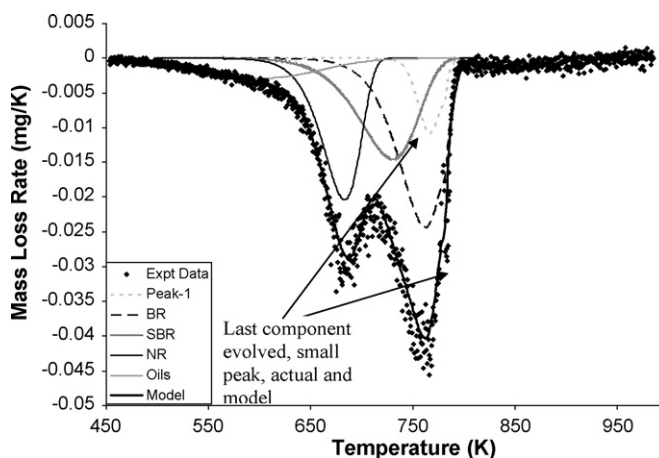

Fig. 4. Deconvolution of tire components for tire brand 1 at dT/dt = 30 K min^{-1}.

Table 3
Frequency factors for tire polymer constituents and respective activation energies.

Type (heating rate)	Oil ($E_a = 43$ kJ mol^{-1})	NR ($E_a = 207$ kJ mol^{-1})	SBRl ($E_a = 152$ kJ mol^{-1})	BR ($E_a = 215$ kJ mol^{-1})
Brand 1 (10 K min^{-1})	13.7 ± 2.3 s^{-1}	$7.68 \pm 8.5 \times 10^{13}$ s^{-1}	$6.90 \pm 7.6 \times 10^{8}$ s^{-1}	$2.94 \pm 3.1 \times 10^{12}$ s^{-1}
Brand 1 (20 K min^{-1})	17.1 ± 2.5 s^{-1}	$1.20 \pm 0.2 \times 10^{14}$ s^{-1}	$1.47 \pm 0.3 \times 10^{9}$ s^{-1}	$7.46 \pm 0.8 \times 10^{12}$ s^{-1}
Brand 1 (30 K min^{-1})	39.3 ± 4.0 s^{-1}	$1.79 \pm 0.2 \times 10^{14}$ s^{-1}	$1.27 \pm 0.2 \times 10^{9}$ s^{-1}	$6.38 \pm 0.7 \times 10^{12}$ s^{-1}
Brand 1 (40 K min^{-1})	58.5 ± 6.0 s^{-1}	$2.15 \pm 0.3 \times 10^{14}$ s^{-1}	$3.26 \pm 0.4 \times 10^{9}$ s^{-1}	$1.52 \pm 0.3 \times 10^{13}$ s^{-1}
Brand 1 (50 K min^{-1})	71.5 ± 6.1 s^{-1*}	$1.97 \pm 0.3 \times 10^{13}$ s^{-1}	$1.00 \pm 0.2 \times 10^{7}$ s^{-1}	$4.47 \pm 0.5 \times 10^{9}$ s^{-1}
Brand 2 (30 K min^{-1})	149 ± 15.5 s^{-1}	$8.41 \pm 0.8 \times 10^{13}$ s^{-1}	$3.26 \pm 0.3 \times 10^{8}$ s^{-1}	$1.93 \pm 0.2 \times 10^{11}$ s^{-1}
Brand 3 (30 K min^{-1})	12.8 ± 1.3 s^{-1}	$2.90 \pm 0.3 \times 10^{14}$ s^{-1}	$6.90 \pm 0.5 \times 10^{8}$ s^{-1}	$5.68 \pm 0.6 \times 10^{13}$ s^{-1}

* At $E_a = 48$ kJ mol^{-1}.

Table 4
Decomposable mass fractions (%).

Type (heating rate)	Oil	NR	SBR	BR	Peak-1	Peak-2
Brand 1 (10 K min^{-1})	15.5 ± 1.6	11.6 ± 1.5	21.6 ± 1.9	51.3 ± 3.5	–	–
Brand 1 (20 K min^{-1})	15.6 ± 1.7	11.1 ± 1.5	22.6 ± 2.1	50.7 ± 4.4	–	–
Brand 1 (30 K min^{-1})	7.9 ± 0.6	16.9 ± 1.7	18.4 ± 2.1	46.4 ± 4.5	10.4 ± 1.0	–
Brand 1 (40 K min^{-1})	5.0 ± 0.7	18.5 ± 1.8	41.9 ± 3.2	32.9 ± 3.3	1.7 ± 0.2	–
Brand 1 (50 K min^{-1})	8.0 ± 0.8	26.6 ± 2.5	19.5 ± 2.5	24.7 ± 2.7	15.1 ± 0.2	6.1 ± 0.3
Brand 2 (30 K min^{-1})	16.7 ± 0.2	28.4 ± 2.3	22.5 ± 2.4	7.6 ± 0.9	14.7 ± 0.2	–
Brand 3 (30 K min^{-1})	16.3 ± 0.2	9.3 ± 1.0	34.3 ± 2.9	29.7 ± 3.0	10.4 ± 0.2	

Table 5
Model fit coefficients and number of data points used.

Type (heating rate)	Data points #	Correlation between Model and data	
		Mass loss rate, dM/dT	Fractional conversion, x
Brand 1 (10 K min^{-1})	2165	0.965	0.997
Brand 1 (20 K min^{-1})	1006	0.982	>0.999
Brand 1 (30 K min^{-1})	795	0.990	0.995
Brand 1 (40 K min^{-1})	800	0.999	>0.999
Brand 1 (50 K min^{-1})	810	0.970	0.997
Brand 2 (30 K min^{-1})	850	0.977	>0.999
Brand 3 (30 K min^{-1})	885	0.990	>0.999

tion of the various compounds that were unable to diffuse to the external surface due to heat and mass transfer limitations. This is due to the difference in the conductivity of the tire material and the ceramic container that holds it [22]. It should be emphasized that such phenomena in tire pyrolysis have not been modeled before. These small peaks in the DTG curve are recorded [7,14] but not successfully modeled. Such a peak cannot be modeled using the conventional approach, and pose an inherent difficulty in decoupling the peaks for many methods presented in literature. A unique method proposed by Kim et al. [10] starts deconvo-

lution by estimating the gradient of the last peak. This method would not be applicable under these high heating rate conditions.

From Table 3, it can be seen that the frequency factors show an overall increase with heating rates, which agree with theoretical considerations that higher energy molecules collide and react more frequently than lower energy ones. Results in Table 3 also agree with past findings in the literature [10,11]. However, higher frequency factors have been reported to increase the difficulty in the pyrolysis reaction [10,11]. Therefore, results derived from the model have implications in the design of a pyrolysis reactor. Results from Table 4
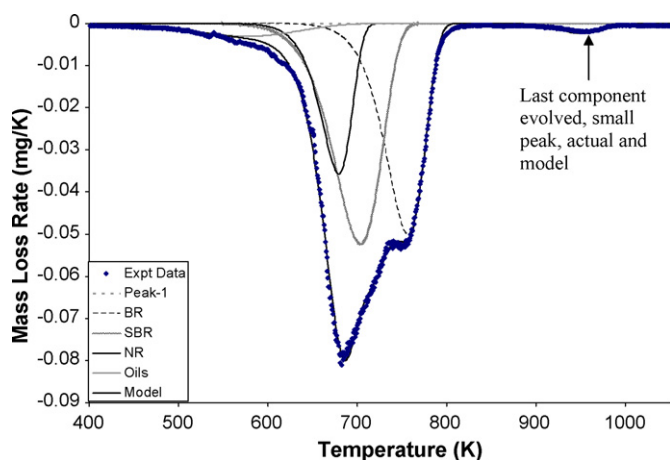

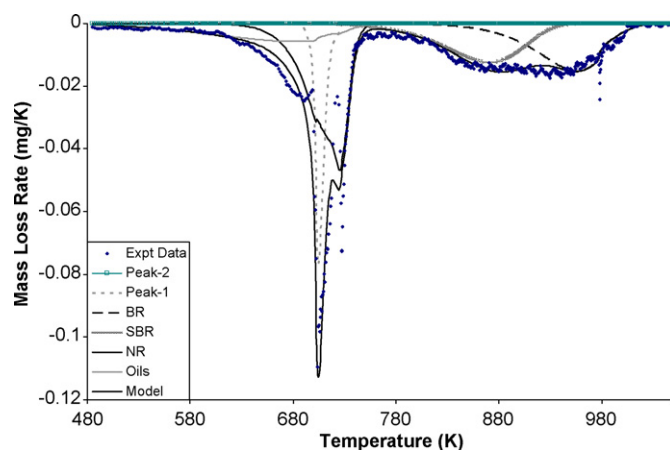Fig. 5. Deconvolution of different components of the tire brand 1 at dT/dt = 40 K min^{-1}.

Fig. 6. Deconvolution of different components of the tire brand 1 at dT/dt = 50 K min^{-1}.
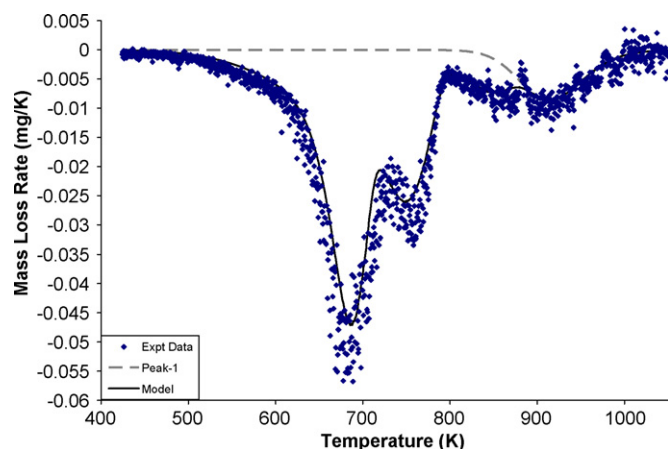
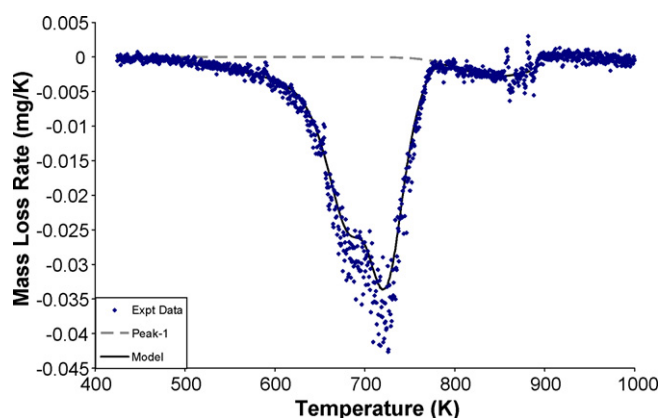**Fig. 7.** DTG curve for the thermal degradation of tire brand 2 at $dT/dt = 30\,K\,min^{-1}$.

Fig. 8. DTG curve for the thermal degradation of tire sample 3 at $dT/dt = 30\,K\,min^{-1}$

also compare well with those of previous studies. For example Kim et al. [10] found oil content of between 11.1–18.3%, 14.8–26.0% for natural rubber and 57.0–70.3% for the man-made elastomers in modeling the pyrolysis of tire tread. They did not decouple the man-made elastomers into SBR and BR portions. In contrast, Seidelt et al. [15] used tire rubber with oil content of between 6% and 37.5% in their modeling efforts.

Although the products from pyrolysis depend on the formulation specific to each brand of tire, the heating rate is also a significant factor [5,6,13,20,27]. Table 4 shows that at higher heating rates (>30 K min^{-1}), both the tire component makeup and the product distribution cannot be accurately determined. Therefore, heat transfer limitations should be avoided in a pyrolytic reactor not only from process control and energy consumption considerations, but also from the quality of the pyrolytic products. The correlation coefficient values (Table 5) also showed that the model parameters are good fits to the various curves. These correlations further validate the model.

For the case of heating rate at 50 K min^{-1}, the heat transfer to the interior of the tire has severely limited the rate of reaction. The rise in the external temperature is too fast for this particular brand of tire that a significant fraction of the mass within the tire could not reach sufficiently high enough temperatures to react. At the molecular level, tire polymer molecules within the tire have not attained sufficient energy to break off from the main polymer chain, until sufficient heat has been conducted through it. This causes the sudden massive spike in Fig. 6 at around 700 K, as a significant number of molecules at this point have obtained sufficient energy for reaction. In fact, the temperature gradient was so great that another smaller peak was recorded at ∼900 K (Fig. 6), requiring the modeling of two distinct peaks due to thermal lag. The thermal lag can also be observed casually in the external temperatures measured at the initiation and completion of tire pyrolysis in Figs 4 and 6. At a low heating rate, the pyrolysis starts at 450 K and ends at 780 K (Fig. 4). However, at a higher heating rate, the pyrolysis starts at 550 K and ends at 1000 K (Fig. 6).

Table 6 shows the kinetic parameters for peaks modeled under the thermal lag conditions. The characteristic time constant shows a decreasing trend with increasing heating rate. This is because conduction of heat to the interior takes a longer time when external temperature rises at a faster rate. This is due to the difference in the conductivity of the tire material and the ceramic container that holds it [22].

The model was also tested with two other brands of tires. Given the above results, the heating rate of 30 K min^{-1} was then applied to two other different brands of tires to further validate the model for thermal lags. The results are shown in Figs. 7 and 8 and Tables 3–6.

Figs 7 and 8 show that the model can also be successfully applied to the DTG curve for a tire with a different formulation (brands 2 and 3) i.e. different NR, SBR and BR components (Table 4). From these results, it can be seen that the model describes the pyrolysis reactions well. Table 5 shows that in these two cases (Figs. 7 and 8), at least 850 data points were used, without modification, and a correlation coefficient of at least 0.977 was obtained. From this exercise, it becomes evident that for heating rates up to 20 K min^{-1}, thermal degradation of rubber tires was all completed well before 780 K (503 °C). Heating rates above 30 K min^{-1} induce a high thermal lag and non-uniform evolution of products.

A limitation of this methodology is that only independent reactions that do not occur simultaneously can be captured by TG measurements and modeled mathematically [28]. Also, apparent characteristic times and activation energies for thermal lag peaks elucidated from these models do not necessarily correspond to 'real' activation energies for any single reaction. The heat and mass transfer consideration is also independent of any reactor geometry, and additional considerations would be required for specific reactor geometries [29,30].

For example, Olazar et al. modeled the pyrolysis kinetics in a conical spouted bed reactor for different tire particle sizes, and concluded that heating rates and heat and mass transfer limitations had a great effect [29]. They further recommend using an efficient laboratory technology for kinetic study due to the sprouted bed gas–solid contact. In this case, an addition of heat and mass transfer equations similar to those in this study could improve the description of tire pyrolysis in the spouted bed reactor. A more in-depth consideration for heat and mass transfer was done by Liu and Jiang for their multilevel reactor [30]. The comprehensive model includes geometrical parameters in separate sets of heat and mass transfer

Table 6
Kinetic constants for thermal lag components.

Type (heating rate)	T_i (s^{-1})	Peak-1	Peak-2
Brand 1 (30 K min^{-1})	$9.88 \pm 1.0 \times 10^{-4}$	$E_a = 583 \pm 62$ kJ mol^{-1}, $A = 6.30 \pm 0.7 \times 10^{49}$ s^{-1}	–
Brand 1 (40 K min^{-1})	$9.84 \pm 1.1 \times 10^{-4}$	$E_a = 536 \pm 73$ kJ mol^{-1}, $A = 6.60 \pm 0.7 \times 10^{39}$ s^{-1}	–
Brand 1 (50 K min^{-1})	$9.74 \pm 1.2 \times 10^{-4}$	$E_a = 418 \pm 68$ kJ mol^{-1}, $A = 7.22 \pm 1.0 \times 10^{33}$ s^{-1}	$E_a = 275 \pm 29$ kJ mol^{-1}, $A = 1.89 \pm 1.0 \times 10^{12}$ s^{-1}
Brand 2 (30 K min^{-1})	$5.99 \pm 6.2 \times 10^{-4}$	$E_a = 129 \pm 13$ kJ mol^{-1}, $A = 3.28 \pm 0.4 \times 10^{7}$ s^{-1}	–
Brand 3 (30 K min^{-1})	$6.28 \pm 6.5 \times 10^{-4}$	$E_a = 77.7 \pm 8.4$ kJ mol^{-1}, $A = 2.56 \pm 0.4 \times 10^{3}$ s^{-1}	–

equations, and was able to elucidate various heat transfer coefficients and temperature of the walls at different levels of the reactor. However, they neglected heat transfer within the individual tire particle. Further consideration of heat conduction within individual particles such as that found in this work could, in principle, improve such elaborate models.

4. Conclusion

In this work, a new mathematical model has been developed to provide insights into the pyrolysis kinetics of tire particles by taking into account both heat and mass transfer processes. The model predictions are consistent with the experimental data obtained at different temperatures, ranging from 450 K to 1000 K. The major conclusion drawn from this work is that the pyrolysis kinetics and the product composition and evolution are highly dependent on the heating rates maintained in the reactor. Specifically, at heating rates beyond $30 \, \text{K min}^{-1}$ there is an abrupt change in the pyrolysis process as revealed by the TGA curves. The model developed in this work together with the derivative thermogravimetric analysis is able to describe accurately the influence of the various kinetic parameters on the pyrolysis reactions at different heating rates. It became further evident that incorporation of heat and mass transfer processes in a pyrolytic model can improve the quantitative understanding of tire pyrolysis, as shown by the better fits of the model results at higher heating rates ($>30 \, \text{K min}^{-1}$). This understanding is particularly important in industrial pyrolysis units from the process control point of view to obtain product(s) with the desired characteristics.

References

[1] Rubber Manufacturers Association (RMA), Scrap Tire Markets in The United States 2005, November 2006.
[2] J.I. Reisman, Air Emissions from Scrap Tire Combustion, EPA-600/R-97-115, October 1997.
[3] E.L.K. Mui, D.C.K. Ko, G. McKay, Production of active carbons from waste tyres––a review, Carbon 42 (2004) 2789–2805.
[4] J.F. Gonzalez, J.M. Encinar, J.L. Canito, J.J. Rodrıguez, Pyrolysis of automobile tyre waste. Influence of operating variables and kinetics study, J. Anal. Appl. Pyrolysis 58–59 (2001) 667–683G.
[5] J.H. Chen, K.S. Chen, L.Y. Tong, On the pyrolysis kinetics of scrap automotive tires, J. Hazard. Mater. B84 (2001) 43–55.
[6] R. Aguado, M. Olazar, D. Vélez, M. Arabiourrutia, J. Bilbao, Kinetics of scrap tyre pyrolysis under fast heating conditions, J. Anal. Appl. Pyrolysis 73 (2005) 290–298.
[7] K. Unapumnuk, T.C. Keener, M. Lu, Pyrolysis Behavior of Tire-Derived Fuels at Different Temperatures and Heating Rates, J. Air Waste Manage. Assoc. 56 (2006) 618–627.
[8] Z. Koreňovaǐ, M. Juma, J. Annus, J. Markoš, Ľ. Jelemensky, Kinetics of pyrolysis and properties of carbon black from a scrap tire, Chem. Pap. 60 (6) (2006) 422–426.
[9] H. Teng, M.A. Serio, M.A. Whjtowicz, R. Bassilakis, P.R. Solomon, Reprocessing of used tires into activated carbon and other products, Ind. Eng. Chem. Res. 34 (1995) 3102–3111.
[10] S. Kim, J.K. Park, H. Chun, Pyrolysis kinetics of scrap tire rubbers I: Using DTG and TGA, J. Environ. Eng. – ASCE 121 (1995) 507–514.
[11] D.Y.C. Leung, C.L. Wang, Kinetic study of scrap tyre pyrolysis and combustion, J. Anal. Appl. Pyrolysis 45 (1998) 153–169.
[12] J.A. Conesa, R. Font, A. Fuliana, J.A. Caballero, Kinetic model for the combustion of tyre wastes, Fuel 77 (13) (1998) 1469–1475.
[13] D.Y.C. Leung, C.L. Wang, Kinetic modeling of scrap tire pyrolysis, Energy Fuels 13 (1999) 421–427.
[14] E. Aylón, M.S. Callen, J.M. Lopez, A.M. Mastral, R. Murillo, M.V. Navarro, S. Stelmach, Assessment of tire devolatilization kinetics, J. Anal. Appl. Pyrolysis 74 (2005) 259–264.
[15] S. Seidelt, M. Muller-Hagedorn, H. Bockhorn, Description of tire pyrolysis by thermal degradation behaviour of main components, J. Anal. Appl. Pyrolysis 75 (2006) 11–18.
[16] R. Murillo, E. Aylón, M.V. Navarro, M.S. Callén, A. Aranda, A.M. Mastral, The application of thermal processes to valorise waste tyre, Fuel Process. Technol. 87 (2006) 143–147.
[17] J.A. Conesa, A. Marcilla, J.A. Caballero, R. Font, Comments on the validity and utility of the different methods for kinetic analysis of thermogravimetric data, J. Anal. Appl. Pyrolysis 58–59 (2001) 617–633.
[18] M. Juma, Z. Koreňovaǐ, J. Markoš, L. Jelemensky, M. Bafrnec, Experimental study of pyrolysis and combustion of scrap tire, Polym. Adv. Technol. 18 (2) (2007) 144–148.
[19] M.P.M. Chinyama, F.C. Lockwood, Devolatilisation behaviour of shredded tyre chips in combusting environment, J. Energy Inst. 80 (3) (2007) 162–167.
[20] J. Yang, P.A. Tanguy, C. Roy, Heat transfer, mass transfer, and kinetics study of the vacuum pyrolysis of a large used tire particle, Chem. Eng. Sci. 30 (1995) 1909–1922.
[21] J. Yang, S. Kaliaguine, C. Roy, Improved quantitative determination of elastomers in tire rubber by kinetic simulation of DTG curves, Rubber Chem. Technol. 66 (1993) 213–229.
[22] J.H. Lienhard IV, J.H. Lienhard V, A Heat Transfer Textbook, Phlogiston Press, Cambridge, Massachusetts, 2008, pp. 22–23.
[23] P.T. William, S. Besler, Pyrolysis-thermogravimetric analysis of tyres and tyre components, Fuel 24 (1995) 1277–1281.
[24] E.M. Suuberg, Y. Sezen, Competitive reaction and transport processes in coal pyrolysis, Proc. 1985 Int. Conf. Coal Sci. (1985) 913–916.
[25] D.L. Pyle, C.A. Zaror, Heat transfer and kinetics in the low temperature pyrolysis of solids, Chem. Eng. Sci. 39 (1984) 147–158.
[26] W.R. Chan, M. Kelbon, B.B. Krieger, Modelling and experimental verification of physical and chemical processes during pyrolysis of a large biomass particle, Fuel 64 (1985) 1505–1513.
[27] J.A. Conesa, R. Font, A. Marcilla, Mass spectrometry validation of a kinetic model for the thermal decomposition of tyre wastes, J. Anal. Appl. Pyrolysis 43 (1997) 83–96.
[28] J.H. Flynn, A. Leo, Wall, General treatment of the thermogravimetry of polymers, J. Res. Natl. Bureau Stand. 70A (1966) 487–522.
[29] M. Olazar, R. Aguado, D. Veïlez, M. Arabiourrutia, J. Bilbao, Kinetics of scrap tire pyrolysis in a conical spouted bed reactor, Ind. Eng. Chem. Res. 44 (11) (2005) 3918–3924.
[30] B.Q. Liu, J.L. Jiang, Mathematical model for mass and heat transfer in multilevel reactor for pyrolysis of used tyres, J. Energy Inst. 79 (3) (2006) 180–186.